Atomic energy levels and Landé g factors: A theoretical study

Wen Huang, Yu Zou, Xiao-Min Tong, and Jia-Ming Li
Institute of Physics, P.O. Box 603, Chinese Academy of Sciences, Beijing 100080, China
(Received 24 February 1995; revised manuscript received 4 May 1995)

We have developed a relativistic multichannel theory that can be used to calculate the multichannel quantum-defect theory parameters $(\mu_\alpha, U_{i\alpha})$ directly from first principles. With the parameters we can calculate the energy levels and Landé g factors of Rydberg series based on the multichannel quantum-defect theory. We have performed calculations of excited states for the Ne atom with major configuration $1s^2 2s^2 2p^5 np$ in $J^\pi = 0^+$, 1^+, 2^+, and 3^+ symmetry. The results are in good agreement with the experimental data. We have also found that the coupling scheme is dependent on the total angular momentum J. The jl-coupling scheme is more suitable than the jj-coupling scheme in describing $J^\pi = 1^+$ symmetry, whereas the jj-coupling scheme is more suitable than the jl-coupling scheme for $J^\pi = 2^+$ symmetry.

PACS number(s): 31.10.+z, 31.50.+w, 31.90.+s

I. INTRODUCTION

In the framework of multichannel quantum-defect theory (MQDT), the properties of an excited atom involving infinite Rydberg states, autoionization states, and adjacent continuum states can be described with a set of physical parameters $(\mu_\alpha, U_{i\alpha})$ [1–12]. The MQDT parameters $(\mu_\alpha, U_{i\alpha})$ can be determined semiempirically by fitting to accurate energy levels and/or other atomic observables from spectroscopic data [8, 10]. However, the numerical fitting procedure requires rather complete spectroscopic data and it then confines the scope of the application of MQDT. In a few cases, the MQDT parameters $(\mu_\alpha, U_{i\alpha})$ were also calculated from first principles under the framework of nonrelativistic theory [9, 12] and the theory of relativistic random phase approximation with exchange (RRPAE) [13].

With the development of relativistic multichannel theory (RMCT) which is a nonperturbative theory and can be applied to any atom (e.g., high-Z atoms), we can calculate the MQDT parameters $(\mu_\alpha, U_{i\alpha})$ from first principles for both bound and continuum energy ranges [14]. RMCT can be regarded as an extension of traditional configuration interaction theory by including continuum configurations. The MQDT parameters $(\mu_\alpha, U_{i\alpha})$ are equivalent to a diagonal representation of the short-range scattering matrix S, namely $S_{ij} = \sum_\alpha U_{i\alpha} \exp(i2\pi\mu_\alpha) U_{j\alpha}$. The energy levels, the Landé g factors, and the coupling schemes can be also obtained with $(\mu_\alpha, U_{i\alpha})$ by means of the MQDT method.

Our RMCT is a full relativistic and nonperturbative method. It should be valid for any atom. To test the method we choose Ne as an example to show our method is valid for a low-Z atom in which the relativistic effects are not important. We have performed calculations of excited states for the Ne atom with major configuration $1s^2 2s^2 2p^5 np$ in $J^\pi = 0^+, 1^+, 2^+$, and 3^+ symmetry. For energy levels of Ne I with $J^\pi = 0^+$, there are strong energy shifts for the states with major $^1S_0$ character the same as the ground state $2p^6\ ^1S_0$ owing to continuum configuration interactions which manifest as "plasma" type radial correlations. In contrast with $^1S_0$, there are negligible energy shifts for the states with major $^3P_0$ character. The results of the energy levels and the Landé g factors for different J^π are in good agreement with the experimental data. The coupling schemes of Ne I for different J^π are also discussed. We find the jl-coupling scheme is more suitable than the jj-coupling scheme in describing $J^\pi = 1^+$ symmetry; the jj-coupling scheme is more suitable than the jl-coupling scheme for $J^\pi = 2^+$ symmetry. We will present our RMCT in Sec. II and calculation results in Sec. III.

II. THEORY

A. Relativistic multichannel theory (RMCT)

We start with a relativistic atomic Hamiltonian H which is obtained by adopting the Coulomb gauge, namely,

$$H\Psi = E\Psi, \tag{1}$$

with

$$H = \sum_i \left(c\vec{\alpha}_i \cdot \vec{p}_i + \beta_i mc^2 - \frac{Ze^2}{r_i} \right) + \sum_{i>j} \frac{e^2}{r_{ij}}. \tag{2}$$

The Breit interactions and the remaining higher-order quantum electrodynamical interactions can be treated as perturbation later and will not be discussed in the present paper. In order to solve Eq. (1), the relativistic atomic Hamiltonian can be recast into (unless otherwise noted, atomic units $m = e = \hbar = 1$ are used)

$$H = H_0 + V, \tag{3}$$

with a relativistic self-consistent field atomic Hamiltonian H_0,

$$H_0 = \sum_i h_i = \sum_i [c\vec{\alpha}_i \cdot \vec{p}_i + \beta_i mc^2 + V_{\mathrm{SCF}}(r_i)] \tag{4}$$

and a residual interaction V,

$$V = \sum_i \left(-\frac{Ze^2}{r_i} - V_{\mathrm{SCF}}(r_i) \right) + \sum_{i>j} \frac{e^2}{r_{ij}}. \quad (5)$$

A relativistic atomic self-consistent-field potential V_{SCF} can be obtained by an atomic self-consistent field (SCF) calculation such as Dirac-Slater SCF with a local exchange approximation [15, 16]. Based on V_{SCF} which is solved for a neutral atom (Ne atom), we can calculate all bound and unbound single-electron wave functions φ_a with combined quantum numbers $a = n\kappa$ or $\varepsilon\kappa$. Thus, they can be used to describe approximately occupied and unoccupied electron orbitals in the atomic system from the point of view of the well-established atomic shell model. From such a complete set of single-electron wave functions, we construct configuration functions Φ_n as antisymmetrized product-type functions of N single-electron wave functions with appropriate angular-momentum couplings and electron occupation distribution. Thus, such configuration functions form bases of the complete Hilbert space for the atomic system with N electrons. Note that we construct the configuration functions through the positive-energy projection operators defined by H_0, thus our method will not suffer from the so-called "Brown-Ravenhall" problem [17, 18]. If we consider the continuum configuration interactions as well as the discrete configuration interactions, wave functions of energy eigenstates can be expressed as [19–21]

$$\Psi(E,i) = \sum_n A_n(E,i)\Phi_n + \sum_j \int_{\epsilon_c} B_{j\epsilon}(E,i)\Phi_{j\epsilon} d\epsilon. \quad (6)$$

The index j refers to various dissociation channels which are various classes of similar configuration functions $\Phi_{j\epsilon}$ with the same core state and different radial excited single-electron orbitals φ [5, 6]. The energy integration can be treated by appropriate energy meshes and starts from ϵ_c (decided according to convenience of computation) above which infinite Rydberg-type configuration functions are treated as channels. More specifically, as illustrated later, first we calculate the MQDT parameters $(\mu_\alpha, U_{i\alpha})$, then the energy levels of infinite Rydberg states above ϵ_c can be obtained from the parameters $(\mu_\alpha, U_{i\alpha})$ in the framework of MQDT. From Eq. (1) and Eq. (6), we can get the following integral equations:

$$E_n^o A_n(E,i) + \sum_{n'} V_{n,n'} A_{n'}(E,i) + \sum_j \int_{\epsilon_c} V_{n,j\epsilon} B_{j\epsilon}(E,i) d\epsilon = E A_n(E,i), \quad (7)$$

$$\sum_n V_{j'\epsilon',n} A_n(E,i) + \epsilon' B_{j'\epsilon'}(E,i) + \sum_j \int_{\epsilon_c} V_{j'\epsilon',j\epsilon} B_{j\epsilon}(E,i) d\epsilon = E B_{j'\epsilon'}(E,i), \quad (8)$$

with $V_{n,n'} = \langle \Phi_n | V | \Phi_{n'} \rangle$, $V_{n,j\epsilon} = \langle \Phi_n | V | \Phi_{j\epsilon} \rangle$, $V_{j'\epsilon',n} = \langle \Phi_{j'\epsilon'} | V | \Phi_n \rangle$, and $V_{j'\epsilon',j\epsilon} = \langle \Phi_{j'\epsilon'} | V | \Phi_{j\epsilon} \rangle$ and E_n^o, ϵ' being the eigenvalues of H_0 corresponding to the eigenfunctions Φ_n and $\Phi_{j'\epsilon'}$. Equation (7) and Eq. (8) can be solved in two cases, namely (1) for discrete eigenenergy corresponding to the first few energy eigenstates of Rydberg series (namely, precursor states) and some finite isolated energy eigenstates with configurations of valence excitations, and (2) for $E \geq \epsilon_c$ (channel treatment aiming directly to calculate the physical parameters μ_α and $U_{i\alpha}$ in MQDT).

For discrete eigenenergy, the $B_{j'\epsilon'}(E,i)$ can be obtained from Eq. (8) (here, the index i is not relevant and can be omitted),

$$B_{j'\epsilon'}(E,i) = \sum_n \hat{G}_E^{-1}(j'\epsilon'; j\epsilon) V_{j\epsilon,n} A_n(E,i), \quad (9)$$

with the coefficients $A_n(E,i)$ and $\hat{G}_E^{-1}(j'\epsilon'; j\epsilon)$ to be calculated. First we can calculate $\hat{G}_E^{-1}(j'\epsilon'; j\epsilon)$ by matrix inversion:

$$\hat{G}_E^{-1}(j'\epsilon'; j\epsilon) \hat{G}_E(j\epsilon; j''\epsilon'') = 1, \quad (10)$$

with

$$\sum_{j'} \int_{\epsilon_c} \hat{G}_E(j\epsilon; j'\epsilon') d\epsilon' = \sum_{j'} \int_{\epsilon_c} [(E-\epsilon)\delta_{j,j'}\delta(\epsilon-\epsilon') - V_{j\epsilon,j'\epsilon'}] d\epsilon'. \quad (11)$$

Then, substituting Eq. (9) into Eq. (7) will lead to an eigenvalue problem,

$$\sum_{n'} \{ (E - E_n^o)\delta_{nn'} - F_{nn'}(E) \} A_{n'}(E,i) = 0, \quad (12)$$

with

$$F_{n,n'}(E) = V_{n,n'} + \sum_j \sum_{j'} \int_{\epsilon_c} d\epsilon' \int_{\epsilon_c} V_{n,j\epsilon} d\epsilon \times \hat{G}_E^{-1}(j\epsilon; j'\epsilon') V_{j'\epsilon',n'}. \quad (13)$$

The first term in Eq. (13) represents discrete-discrete configuration interaction and the second is the discrete-continuum interaction. The CI without continuum calculation only takes the first term into account and omits the discrete-continuum interaction term. The importance of the discrete-continuum interaction will be demonstrated later (Table I). The discrete eigenenergy E_n can be calculated by adjusting the coefficient determinant in Eq. (12) equal to zero. Here we adopt a frozen core approximation and set the energy zero at the first ionization threshold corresponding to the ionic state $(2p^5\ {}^2P^o_{3/2})$.

At $E \geq \epsilon_c$ lies the energy region where infinite Rydberg discrete states, autoionization states, and continuum states are treated in a unified manner by MQDT. The $B_{j'\epsilon'}(E,i)$ can be expressed as

$$B_{j'\epsilon'}(E,i) = \left[\mathcal{P} \frac{K_{j'\epsilon',iE}}{(E-\epsilon')} + \delta_{j'i}\delta(\epsilon'-E) \right] D(E,i), \quad (14)$$

with the unknown $K_{j'\epsilon',iE}$ to be calculated and the normalization factors $D(E,i)$ to be determined by asymptotic boundary conditions. The $\mathcal{P}$ represents principal integration. Similarly, we can get

$$A_n(E,i) = \frac{K_{n,iE}}{E - E_n^o} D(E,i). \tag{15}$$

By substituting Eq. (14) and Eq. (15) into Eq. (7) and Eq. (8), it leads to a Lippmann-Schwinger-type integral equation [22, 23],

$$K_{n',iE} = V_{n',iE} + \sum_j \int_{\epsilon_c} \frac{V_{n',j\epsilon} K_{j\epsilon,iE}}{E - \epsilon} d\epsilon + \sum_n \frac{V_{n',n} K_{n,iE}}{E - E_n^o}, \tag{16}$$

$$K_{j'\epsilon',iE} = V_{j'\epsilon',iE} + \sum_j \int_{\epsilon_c} \frac{V_{j'\epsilon',j\epsilon} K_{j\epsilon,iE}}{E - \epsilon} d\epsilon + \sum_n \frac{V_{j'\epsilon',n} K_{n,iE}}{E - E_n^o}. \tag{17}$$

The $K_{j\epsilon,iE}$ and $K_{n,iE}$ matrix can be calculated by solving Eq. (16) and Eq. (17). After getting the $K_{j\epsilon,iE}$ matrix, the energy eigenstate wave functions in Eq. (6) have the following asymptotic expressions:

$$\Psi(E,i) \overset{r\to\infty}{\longrightarrow} \left[\Phi_{iE} + \sum_j \tilde{\Phi}_{iE}(-\pi K_{jE,iE})\right] D(E,i) \overset{r\to\infty}{\longrightarrow} \mathcal{A}\left\{\sum_j \Theta_j [f_j(r,E)\mathcal{C}_{ji} - g_j(r,E)\mathcal{S}_{ji}] D(E,i)\right\}, \tag{18}$$

where

$$\Phi_{iE} \overset{r\to\infty}{\longrightarrow} \mathcal{A}\{\Theta_i[f_i(r,E)\cos(\pi\mu_i^o) - g_i(r,E)\sin(\pi\mu_i^o)]\}, \tag{19}$$

$$\tilde{\Phi}_{iE} \overset{r\to\infty}{\longrightarrow} \mathcal{A}\{\Theta_i[-f_i(r,E)\sin(\pi\mu_i^o) + g_i(r,E)\cos(\pi\mu_i^o)]\}, \tag{20}$$

$$\mathcal{C}_{ji} = \delta_{ji}\cos(\pi\mu_j^o) + \pi K_{ji}\sin(\pi\mu_j^o), \tag{21}$$

$$\mathcal{S}_{ji} = \delta_{ji}\sin(\pi\mu_j^o) - \pi K_{ji}\cos(\pi\mu_j^o), \tag{22}$$

with $K_{ji} = K_{jE,iE}$. Here, $\mathcal{A}$ is the antisymmetrization operator. Θ_i is the product-type wave function of the core-state wave function and the angular wave function of the excited electron. The f_i and g_i are regular and irregular relativistic Coulombic functions [5]. The μ_i^o is the quantum defect (namely, short-range phase shift in a unit of π) of the ith channel which has been obtained by the calculation based on $V_{\rm SCF}$. The normalization factor $D_\alpha(E,i)$ are determined such that eigenchannel wave functions are satisfied with the following boundary conditions:

$$\Psi_\alpha \overset{r\to\infty}{\longrightarrow} \sum_i \Psi_{iE} \overset{r\to\infty}{\longrightarrow} \mathcal{A}\left\{\sum_i \sum_j \Theta_j [f_j(r,E)\mathcal{C}_{ji} - g_j(r,E)\mathcal{S}_{ji}] D_\alpha(E,i)\right\} \overset{r\to\infty}{\longrightarrow} \mathcal{A}\left\{\sum_j \Theta_j U_{j\alpha}[f_j(r,E)\cos(\pi\mu_\alpha) - g_j(r,E)\sin(\pi\mu_\alpha)]\right\}, \tag{23}$$

with the α denoting the αth eigenchannel. The $\tan(\pi\mu_\alpha)$ and the $U_{j\alpha}$ are the eigenvalues and the corresponding eigenvectors of $\mathcal{C}^{-1}\mathcal{S}$ matrix with the $\mathcal{C}$ matrix in Eq. (21) and the $\mathcal{S}$ matrix in Eq. (22), namely,

$$\sum_k (\mathcal{C}^{-1})_{jk}\mathcal{S}_{ki} = \sum_\alpha U_{j\alpha}\tan(\pi\mu_\alpha)U_{i\alpha}, \tag{24}$$

where the μ_α are the eigenquantum defects and the orthogonal matrix $U_{i\alpha}$ is the transformation matrix in MQDT. With the parameters $(\mu_\alpha, U_{i\alpha})$ we can calculate the atomic energy levels and properties by the following MQDT method.

B. MQDT calculation of atomic energy levels, Landé g factors, and coupling schemes

In MQDT the energy eigenfunction of an excited atom can be written as a superposition of the eigenchannel wave functions, i.e.,

$$\Psi = \sum_\alpha \Psi_\alpha A_\alpha, \tag{25}$$

where Ψ_α satisfies the asymptotic boundary condition Eq. (23). The MQDT parameters $(\mu_\alpha, U_{i\alpha})$ in Eq. (23) are expected to vary smoothly with the energy. For bound states the asymptotic boundary conditions lead to the linear equations

$$\sum_\alpha [U_{i\alpha} \sin \pi(\nu_i + \mu_\alpha)] A_\alpha = 0, \tag{26}$$

where ν_i satisfies

$$(I_i - E)\,\alpha^2 = 1 - \left\{ 1 + \frac{\alpha^2 (q+1)^2}{\left[\sqrt{\kappa^2 - \alpha^2(q+1)^2} + \nu_i - |\kappa|\right]^2} \right\}^{-1/2} \quad \text{for all } i. \tag{27}$$

Here, I_i is the ionization threshold of the atom corresponding to the ith ionization channel; q is the degree of ionization. In the nonrelativistic limit we have $\nu_i = (q+1)/\sqrt{2(I_i - E)}$. To obtain nonzero solutions of A_α, the determinant of the coefficient matrix of Eq. (26) must be equal to zero. It then generates innumerable discrete energy levels. The mixing coefficients A_α can be calculated by Eq. (2.11) in [9].

The operator g is diagonal in LS-coupling representation, i.e.,

$$g_{(LS)} = [3J(J+1) - L(L+1) + S(S+1)]/[2J(J+1)]. \tag{28}$$

Thus we set up a transformation between the eigenchannel (α) representation and the LS-coupling (LS) representation. The transformation matrix can be obtained by $U_{(LS),\alpha} = \sum_i V_{(LS),i}\, U_{i\alpha}$. Here $V_{(LS),i}$ transforms the jj-coupling ionization channels (i) into the LS-coupling channels (LS). The Landé g factor is then obtained by

$$\langle g \rangle = \sum_{(LS)} g_{(LS)} \left(\sum_\alpha U_{(LS),\alpha} A_\alpha \right)^2 \quad \text{with } \sum_\alpha (A_\alpha)^2 = 1. \tag{29}$$

Thus the energy levels and Landé g factors can be calculated when $(\mu_\alpha, U_{i\alpha})$ are known. In practice, because $(\mu_\alpha, U_{i\alpha})$ are expected to vary smoothly with the energy, we calculate $(\mu_\alpha, U_{i\alpha})$ only at a few energy points with RMCT and get the values of $(\mu_\alpha, U_{i\alpha})$ for any energy point by means of linear extrapolation or interpolation. An orthogonal matrix U can be expressed by means of $n(n-1)/2$ Euler's angles θ_{lm} with a conventional sequence,

$$U = \prod_{i=1}^{n-1} \prod_{j=n}^{i+1} R^{lm}(\theta_{lm}), \tag{30}$$

where $R^{lm}(\theta_{lm})$ is an n-dimensional orthogonal matrix which defers from unit matrix by replacing (ll)th, (lm)th, (ml)th, and (mm)th elements with $\cos\theta_{lm}$, $-\sin\theta_{lm}$, $\sin\theta_{lm}$, and $\cos\theta_{lm}$, respectively [8]. Thus the extrapolation or interpolation on $U_{i\alpha}$ is obtained through that on Euler's angles θ_{lm}.

With $(\mu_\alpha, U_{i\alpha})$ we can also calculate the percentages of different jj-coupling, jl-coupling, and LS-coupling channels in each energy level by means of representation transformation, i.e.,

$$(A_q)^2 = \left(\sum_\alpha U_{q,\alpha} A_\alpha \right)^2 \quad \text{with } \sum_\alpha (A_\alpha)^2 = 1, \tag{31}$$

where $q = i(jj\text{-coupling})$, $jl(jl\text{-coupling})$, or $LS(LS\text{-coupling})$.

III. CALCULATION RESULTS AND DISCUSSION

A. $J^\pi = 0^+$

Table I gives out the calculated eigenenergy E_n with respect to the first ionization threshold. The results are obtained by adjusting the coefficient determinant in Eq. (12) equal to zero. To demonstrate the importance of the continuum configuration, we also calculate eigenenergy $E_n^{(1)}$ of a few low-lying excited states and the corresponding wave functions, according to the CI without continuum method which only involves bound-type configuration functions with principal quantum number less than 6. The difference between E_n and $E_n^{(1)}$ represents an energy shift owing to continuum configuration interactions. It is interesting to note that the energies E_n of $np\ [\frac{1}{2}]_0$ have negligible energy shifts while the energies of E_n of $np'\ [\frac{1}{2}]_0$ have larger energy shifts. The

TABLE I. Energy levels (in a.u.) for Ne in the $J^\pi = 0^+$ symmetries. E_n^o, $E_n^{(1)}$, and E_n are from the calculation of the Dirac-Slater SCF, the CI without continuum, and the relativistic multichannel theory, respectively.

Energy level	E_n^o	$E_n^{(1)}$	E_n	$E_{\rm exp}$ [24]
$2p^6\ {}^1S_0$	-0.7336	-0.6931	-0.7946	-0.7925
$2p^5(^2P^o_{1\frac{1}{2}})3p\ [\frac{1}{2}]_0$	-0.1046	-0.1042	-0.1029	-0.1049
$2p^5(^2P^o_{1\frac{1}{2}})3p'\ [\frac{1}{2}]_0$	-0.1004	-0.0792	-0.0931	-0.0955
$2p^5(^2P^o_{1\frac{1}{2}})4p\ [\frac{1}{2}]_0$	-0.0488	-0.0470	-0.0474	-0.0480
$2p^5(^2P^o_{1\frac{1}{2}})4p'\ [\frac{1}{2}]_0$	-0.0445	-0.0361	-0.0432	-0.0439
$2p^5(^2P^o_{1\frac{1}{2}})5p\ [\frac{1}{2}]_0$	-0.0282	-0.0259	-0.0273	-0.0276
$2p^5(^2P^o_{1\frac{1}{2}})5p'\ [\frac{1}{2}]_0$	-0.0239	-0.0090	-0.0240	-0.0243

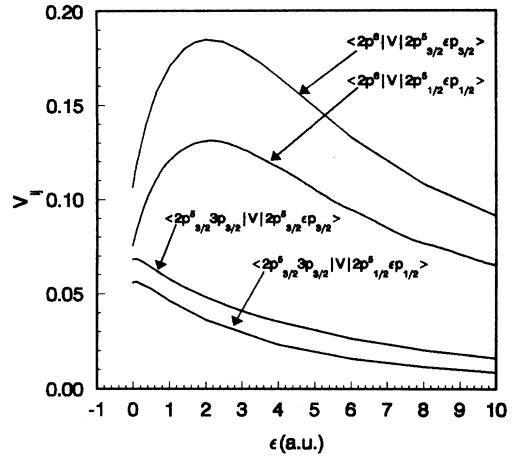

FIG. 1. Residual interaction matrix elements V_{ij} for $J^\pi = 0^+$ symmetry.

$np\ [\frac{1}{2}]_0$ states have major components with $^3P_0$ character, while the $np'\ [\frac{1}{2}]_0$ states have major components with $^1S_0$ character, the same as the ground state $2p^6\ ^1S_0$. In order to elucidate the continuum configuration interactions, we display the residual interaction matrix elements V_{ij} as shown in Fig. 1. For the residual interaction matrix elements between the ground-state configuration $2p^6$ and the channel configurations $2p^5np/\epsilon p$, a very narrow energy domain just below the zero (the first ionization threshold) contains infinite bound configurations $2p^5np$ and there is a "resonant peak" in the continuum state energy range which can be regarded as radial "plasma" type correlation due to the following understanding [25]. There are six $2p$ electrons in the ground state of a Ne atom which form spherical symmetric electronic cloud. If we treat the spherical symmetric electronic cloud as a plasma, the plasma frequency can be calculated as $\omega = \langle 2p|(4\pi n_e e^2/m_e)^{1/2}|2p\rangle$=3.0 (a.u.), where n_e is the density of the electronic cloud. If one of the $2p$ electrons is excited, the dominant collective correlation should be corresponding to "classic plasma oscillation." Therefore, the difference of the peak position of the residual interaction and the $2p$ orbital energy should be around the plasma oscillation energy $\hbar\omega$, i.e., 3.0 a.u. As shown in Fig. 1, the difference is 2.8 a.u., which is quite close to our predicted plasma oscillation energy (3.0 a.u.). In Fig. 1 there is no peak for the residual interaction matrix elements between the first excited state configuration $2p^5_{3/2}3p_{3/2}$ and the channel configurations $2p^5np/\epsilon p$. The phenomenon can be also understood based on the

TABLE II. Eigenquantum defect μ_α and transformation matrix $U_{i\alpha}$ for $J^\pi = 0^+$ symmetry ($\epsilon = -0.0186$ a.u.).

	α	^1S	^3P
i	$\mu_i^o \setminus \mu_\alpha$	0.676	0.800
$2p^5(^2P_{3/2})\epsilon p_{3/2}$	0.820	0.933	-0.360
$2p^5(^2P_{1/2})\epsilon p_{1/2}$	0.820	0.360	0.933

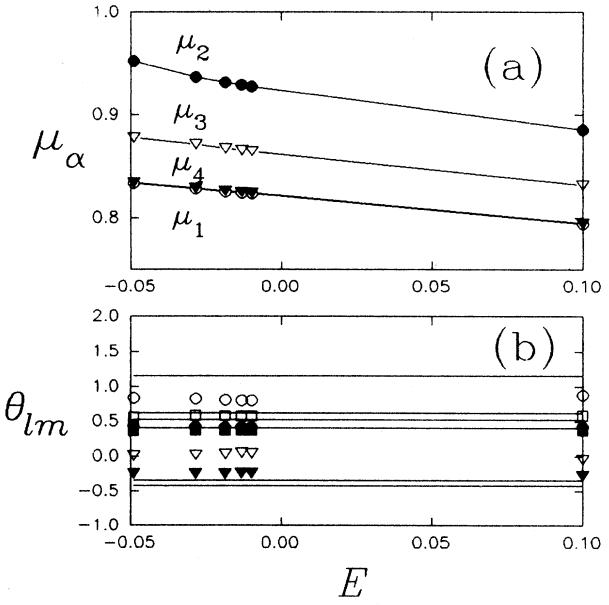

FIG. 2. The quantum defects μ_α and Euler's angles θ_{lm} of $U_{i\alpha}$ for $J^\pi = 1^+$ symmetry of a Ne atom. The respective Euler's angles of the transformation matrix between LS-coupling and jj-coupling channels are also given with the solid lines. Euler's angles are θ_{12}, θ_{24}, θ_{13}, θ_{34}, θ_{14}, and θ_{23} from the largest to the smallest. The jj-coupling channels are $(3/2,1/2)_1, (3/2,3/2)_1, (1/2,1/2)_1$, and $(1/2,3/2)_1$ in sequence. The LS-coupling channels are $^1P_1$, $^3S_1$, $^3D_1$, and $^3P_1$ in sequence.

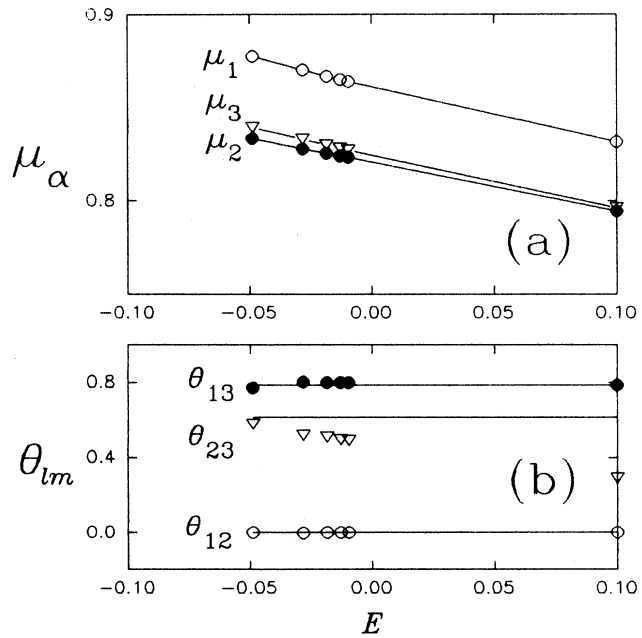

FIG. 3. The quantum defects μ_α and Euler's angles θ_{lm} of $U_{i\alpha}$ for $J^\pi = 2^+$ symmetry of the Ne atom. The respective Euler's angles of the transformation matrix between LS-coupling and jj-coupling channels are also given with the solid lines. The jj-coupling channels are $(3/2,1/2)_2, (3/2,3/2)_2$, and $(1/2,3/2)_2$ in sequence. The LS-coupling channels are $^3D_2$, $^3P_2$, and $^1D_2$ in sequence.

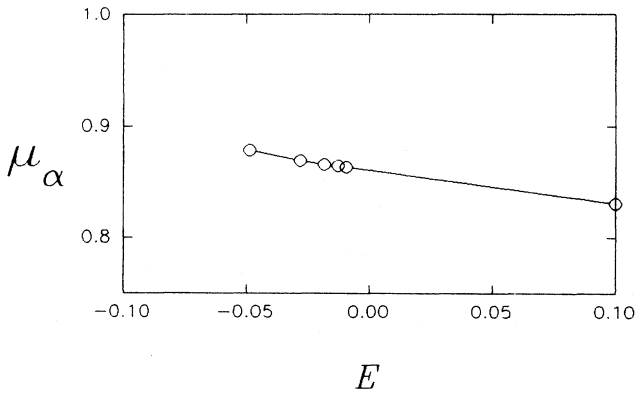

FIG. 4. The quantum defect μ_α for $J^\pi = 3^+$ symmetry of a Ne atom.

"plasma" type correlation. When the $3p$ electron is excited, it will be excited to np or ϵp orbit. In such a case, only one electron is in the $3p$ orbit and there is not collective correlation. Thus for such a quantum system containing limited electrons it is worthwhile studying the collective correlation based on the physical picture of the independent electronic motion.

Table II lists the eigenquantum defects and the transformation matrix of Ne in $J^\pi = 0^+$ symmetry. The calculated eigenquantum defects are in good agreement with the values obtained by fitting to observed energy levels, i.e., 0.679 and 0.807 [26].

B. $J^\pi = 1^+, 2^+, 3^+$

Figures 2 and 3 show the calculated results of μ_α and θ_{lm} of $U_{i\alpha}$ for $J^\pi = 1^+$ and 2^+ symmetry of

TABLE III. Excited energy (cm^{-1}), Landé g factor, and percentage of predominant channel in various coupling schemes of Ne I bound state in J^π=1^+, 2^+, and 3^+ symmetry. $np\ [K]_J$ denotes $2p^5(^2P^o_{3/2})np\ [K]_J$, $np'\ [K]_J$ denotes $2p^5(^2P^o_{1/2})np\ [K]_J$. The predominant channels are indicated with the labels in the parentheses, i.e., (i) for $J^\pi = 1^+$, (1), (2), (3), and (4) denote $2p^5(^2P^o_{3/2})np_{1/2}/\epsilon p_{1/2}$ $(3/2,1/2)_1$, $2p^5(^2P^o_{3/2})np_{3/2}/\epsilon p_{3/2}$ $(3/2,3/2)_1$, $2p^5(^2P^o_{1/2})np_{1/2}/\epsilon p_{1/2}$ $(1/2,1/2)_1$, and $2p^5(^2P^o_{1/2})np_{3/2}/\epsilon p_{3/2}$ $(1/2,3/2)_1$ for jj-coupling, $2p^5(^2P^o_{3/2})np/\epsilon p$ $[3/2]_1$, $2p^5(^2P^o_{3/2})np/\epsilon p$ $[1/2]_1$, $2p^5(^2P^o_{1/2})np/\epsilon p$ $[3/2]_1$, and $2p^5(^2P^o_{1/2})np/\epsilon p$ $[1/2]_1$ for jl-coupling, $^1P_1$, $^3S_1$, $^3D_1$, and $^3P_1$ for LS-coupling scheme; (ii) for $J^\pi = 2^+$, (1), (2), and (3) denote $2p^5(^2P^o_{3/2})np_{1/2}/\epsilon p_{1/2}$ $(3/2,1/2)_2$, $2p^5(^2P^o_{3/2})np_{3/2}/\epsilon p_{3/2}$ $(3/2,3/2)_2$, and $2p^5(^2P^o_{1/2})np_{3/2}/\epsilon p_{3/2}$ $(1/2,3/2)_2$ for jj-coupling, $2p^5(^2P^o_{3/2})np/\epsilon p$ $[5/2]_2$, $2p^5(^2P^o_{3/2})np/\epsilon p$ $[3/2]_2$, and $2p^5(^2P^o_{1/2})np/\epsilon p$ $[3/2]_2$ for jl-coupling, $^3D_2$, $^3P_2$, and $^1D_2$ for LS-coupling scheme.

Desig.	E_{th}	E_{expt}[24]	g_{th}	g_{expt}[24]	Percentage of predominant channel		
					jj-coupling	jl-coupling	LS-coupling
$3p\ [\frac{1}{2}]_1$	146 419	148 260	1.981	1.984	(2)0.445	(2) 0.816	(1)0.970
$3p\ [\frac{3}{2}]_1$	149 602	150 124	0.625	0.669	(3)0.372	(1) 0.583	(2)0.812
$3p'\ [\frac{3}{2}]_1$	150 516	150 774	1.027	0.999	(3)0.540	(3) 0.605	(4)0.534
$3p'\ [\frac{1}{2}]_1$	150 827	151 040	1.356	1.340	(4)0.731	(4) 0.820	(3)0.649
$4p\ [\frac{1}{2}]_1$	162 240	162 520	1.944	1.929	(2)0.499	(2) 0.901	(1)0.915
$4p\ [\frac{3}{2}]_1$	162 908	163 015	0.943	0.974	(1)0.533	(1) 0.961	(4)0.442
$4p'\ [\frac{3}{2}]_1$	163 532	163 659	0.709	0.685	(3)0.866	(3) 0.969	(2)0.684
$4p'\ [\frac{1}{2}]_1$	163 619	163 710	1.405	1.397	(4)0.823	(4) 0.921	(3)0.600
$5p\ [\frac{1}{2}]_1$	167 374	167 451	1.868		(2)0.540	(2) 0.976	(1)0.802
$5p\ [\frac{3}{2}]_1$	167 602	167 642	1.022		(1)0.551	(1) 0.996	(4)0.523
$5p'\ [\frac{3}{2}]_1$	168 300	168 357	0.631		(3)0.902	(3) 0.997	(2)0.796
$5p'\ [\frac{1}{2}]_1$	168 314	168 361	1.493		(4)0.893	(4) 0.987	(3)0.520
$3p\ [\frac{5}{2}]_2$	149 231	149 826	1.159	1.137	(1) 0.846	(1) 0.706	(1) 0.858
$3p\ [\frac{3}{2}]_2$	150 105	150 318	1.271	1.229	(2) 0.976	(2) 0.764	(2) 0.540
$3p'\ [\frac{3}{2}]_2$	150 718	150 860	1.231	1.301	(3) 0.836	(3) 0.836	(3) 0.441
$4p\ [\frac{5}{2}]_2$	162 782	162 901	1.151	1.112	(1) 0.966	(1) 0.819	(1) 0.670
$4p\ [\frac{3}{2}]_2$	162 974	163 040	1.338	1.360	(2) 0.996	(2) 0.840	(2) 0.677
$4p'\ [\frac{3}{2}]_2$	163 629	163 711	1.174	1.184	(3) 0.975	(3) 0.975	(3) 0.420
$5p\ [\frac{5}{2}]_2$	167 553	167 593	1.147		(1) 0.992	(1) 0.844	(1) 0.565
$5p\ [\frac{3}{2}]_2$	167 623	167 651	1.349		(2) 0.996	(2) 0.847	(2) 0.699
$5p'\ [\frac{3}{2}]_2$	168 341	168 381	1.168		(3) 0.997	(3) 0.997	(1) 0.450
$3p\ [\frac{5}{2}]_3$	148 865	149 659	1.333	1.329			
$4p\ [\frac{5}{2}]_3$	162 660	162 833	1.333	1.328			
$5p\ [\frac{5}{2}]_3$	167 498	167 561	1.333				

a Ne atom. $U_{i\alpha}$ can be obtained from Eq. (30), where i denotes the jj-coupling channel, i.e., i=1, 2, 3, and 4 denote $2p^5(^2P^o_{3/2})np_{1/2}/\epsilon p_{1/2}$ $(3/2,1/2)_1$, $2p^5(^2P^o_{3/2})np_{3/2}/\epsilon p_{3/2}$ $(3/2,3/2)_1$, $2p^5(^2P^o_{1/2})np_{1/2}/\epsilon p_{1/2}$ $(1/2,1/2)_1$ and $2p^5(^2P^o_{1/2})np_{3/2}/\epsilon p_{3/2}$ $(1/2,3/2)_1$ for $J^\pi = 1^+$, i=1, 2, and 3 denote $2p^5(^2P^o_{3/2})np_{1/2}/\epsilon p_{1/2}$ $(3/2,1/2)_2$, $2p^5(^2P^o_{3/2})np_{3/2}/\epsilon p_{3/2}$ $(3/2,3/2)_2$, and $2p^5(^2P^o_{1/2})np_{3/2}/\epsilon p_{3/2}$ $(1/2,3/2)_2$ for $J^\pi = 2^+$; α denotes the eigenchannel. The respective Euler's angles of the transformation matrix $W_{i,(LS)}$ from LS-coupling to jj-coupling channels are also given out with the solid lines, where (LS) = 1, 2, 3, and 4 denote $^1P_1$, $^3S_1$, $^3D_1$, and $^3P_1$ for $J^\pi = 1^+$; (LS) = 1, 2, and 3 denote $^3D_2$, $^3P_2$, and $^1D_2$ for $J^\pi = 2^+$. It can be seen that the eigenchannels are basically the LS-coupling channels with the same labels. Figure 4 shows the calculated results of μ_α of $J^\pi = 3^+$ symmetry for which only one channel is involved. Both μ_α and θ_{lm} for different symmetry vary smoothly with the energy.

Table III displays some calculated results of the energy levels and Landé g factors of a Ne atom for $J^\pi = 1^+, 2^+$, and 3^+ with the MQDT parameters $(\mu_\alpha, U_{i\alpha})$. In our calculation the experimental ionization thresholds I_i are used. The similar calculated results can be easily obtained for the other higher Rydberg series. The Landé g factors as well as the energy levels are in good agreement with the experimental data.

Table III also displays the calculated percentages of the predominant channels in jj-coupling, jl-coupling, and LS-coupling schemes for each energy level. Traditionally the jl-coupling scheme is used to describe the excited states of rare-gas atoms. It is suitable for a Ne atom with $J^\pi = 1^+$ symmetry, except for some levels which tend to be LS-coupled. Nevertheless, the jj-coupling scheme proves to be a more favorable one for a Ne atom with $J^\pi = 2^+$ symmetry. It reveals different dynamic properties between $J^\pi = 1^+$ and $J^\pi = 2^+$ symmetry, although they have the same electronic configuration. Such a difference implies that a Ne atom with a larger total angular momentum for the same electronic configuration has a weaker interaction between the atomic core and the excited electron, and thus tends to possess more character of jj-coupling.

In Table III we can see that there are four Rydberg series of a Ne atom with $J^\pi = 1^+$ and three Rydberg series with $J^\pi = 2^+$. The Rydberg series are strongly disturbed. Especially, the disturbance greatly influences the Landé g factors and has caused large variation of the values and the sequence of g among the Rydberg series when the principle quantum number varies. For example, in $np[\frac{3}{2}]_1$ series, g factors are equal to 0.669, 0.974, ... as $n = 3, 4, \ldots$, which can be described precisely by MQDT. Such disturbance also influences the coupling schemes. For example, $3p[\frac{3}{2}]_1$ is LS-coupled, whereas $4p[\frac{3}{2}]_1$ is jl-coupled.

IV. CONCLUSION

In conclusion, MQDT offers a powerful method to describe the properties of excited atoms. The development of RMCT offers us an effective method which can accurately calculate the physical parameters $(\mu_\alpha, U_{i\alpha})$ in MQDT. The calculation presented in this paper can be extended to any atom with different J^π symmetry. With the recent development of precision laser spectroscopy, there will be a wealth of accurate spectroscopic data available for complex atoms (e.g., Ru,Yb,Dy) [27]. Thus the semiempirical analysis combined with the new development of RMCT will offer us very accurate data of the physical parameters $(\mu_\alpha, U_{i\alpha})$. Through the intimate relationship between bound and continuum states in the framework of MQDT, accuracy of the collision cross sections can be tested by the experimental results (e.g., energy levels and Landé g factors) obtained from the most accurate experimental spectroscopic data. This should be very useful for future studies of electronic collisions with atomic ions.

ACKNOWLEDGMENTS

This work was partially supported by the Chinese Association of Atomic and Molecular Data, SSTCC, Science and Technology Funds of CAEP, National High-Tech ICF Committee in China, and the National Natural Science Foundation of China.

[1] M. J. Seaton, Proc. Phys. Soc. London **88**, 801 (1966).
[2] M. J. Seaton, Rep. Prog. Phys. **46**, 167 (1983).
[3] U. Fano, Phys. Rev. A **2**, 353 (1970).
[4] U. Fano, J. Opt. Soc. Am. **65**, 979 (1975).
[5] C. M. Lee (Jia-Ming Li) and W. R. Johnson, Phys. Rev. A **22**, 979 (1980).
[6] Jia-Ming Li, Acta Phys. Sin. **29**, 419 (1980).
[7] Jia-Ming Li, Acta Phys. Sin. **32**, 84 (1983).
[8] C. M. Lee (Jia-Ming Li) and K. T. Lu, Phys. Rev. A **8**, 1241 (1973).
[9] C. M. Lee (Jia-Ming Li), Phys. Rev. A **10**, 584 (1974).
[10] M. Aymar, Phys. Rep. **110**, 163 (1984).
[11] C. Greene, U. Fano, and G. Strinati, Phys. Rev. A **19**, 1485 (1979).
[12] C. H. Greene and L. Kim, Phys. Rev. A **36**, 2706 (1987).
[13] W. R. Johnson, K. T. Cheng, K.-N. Huang, and M. Le Dourneuf, Phys. Rev. A **22**, 989 (1980).
[14] Yu Zou, Xiao-Ming Tong, and Jia-Ming Li (unpublished).
[15] D. A. Libermann, D. T. Comer, and J. T. Waber, Comput. Phys. Commun. **2**, 107 (1971).
[16] Jia-Ming Li and Zhong-Xin Zhao, Acta Phys. Sin. **31**, 97 (1982).
[17] G. E. Brown and D. G. Ravenhall, Proc. R. Soc. London Ser. A **208**, 552 (1951).
[18] J. Sucher, Phys. Rev. A **22**, 348 (1980).
[19] U. Fano, Phys. Rev. **124**, 1866 (1961).
[20] Jia-Ming Li, Ying-Jian Wu, and R. H. Pratt, Phys. Rev. A **40**, 3036 (1989).

[21] Ying-Jian Wu and Jia-Ming Li, Acta Phys. Sin. **38**, 1056 (1989).
[22] U. Fano and F. Prats, Proc. Natl. Acad. Sci. (India) A **33**, 553 (1963).
[23] A. F. Starace, in *Handbuch der Physics* (Springer, Berlin, 1982), Vol. 31, pp. 1–121.
[24] C. E. Moore, in *Atomic Energy Levels*, Natl. Bur. Stand. (U.S.) No. 35 (U.S. GPO, Washington, D.C., 1971), Vol. 1, pp. 76–82.
[25] Yu Zou, Xiao-Min Tong, and Jia-Ming Li, Acta Phys. Sin. **44**, 50 (1995).
[26] A. F. Starace, J. Phys. B **6**, 76 (1973).
[27] X. Y. Xu *et al.*, J. Phys. B **23**, 3315(1990); P. Camus *et al.*, *ibid.* **13**, 1073 (1980); H. J. Zhou *et al.*, Acta Phys. Sin. (Overseas Edition) **1**, 19 (1992); C. B. Xu *et al.*, J. Phys. B **27**, 3905 (1994).